Critical roles of the guanylyl cyclase B receptor in endochondral ossification and development of female reproductive organs

Naohisa Tamura*†, Lynda K. Doolittle*†‡, Robert E. Hammer*‡§, John M. Shelton¶, James A. Richardson‖, and David L. Garbers*†‡**

*Cecil H. and Ida Green Center for Reproductive Biology Sciences, Departments of †Pharmacology, §Biochemistry, and ‖Pathology and Molecular Biology, ¶Department of Internal Medicine, Cardiology Division, and ‡Howard Hughes Medical Institute, University of Texas Southwestern Medical Center, Dallas, TX 75390

Contributed by David L. Garbers, October 24, 2004

Guanylyl cyclase B is the receptor for a small peptide (C-type natriuretic peptide) produced locally in many different tissues. To unravel the functions of the receptor, we generated mice lacking guanylyl cyclase B through gene targeting. Expression of the receptor mRNA in tissues such as bone and female reproductive organs was evident, and significant phenotypes associated with each of these tissues were apparent in null mice. A dramatic impairment of endochondral ossification and an attenuation of longitudinal vertebra or limb-bone growth were seen in null animals. C-type natriuretic peptide-dependent increases of guanylyl cyclase B activity, but not basal enzyme activity, appeared to be required for the progression of endochondral ossification. Female mice were infertile, but male mice were not. This result was due to the failure of the female reproductive tract to develop. Thus, the guanylyl cyclase B receptor is critical for the development of both bone and female reproductive organs.

C-type natriuretic peptide | cyclic GMP | female reproduction | skeletal growth

The mammalian guanylyl cyclase (GC) family of receptors consists of GCs containing a single-transmembrane segment and those containing no apparent transmembrane regions (1). Seven single-transmembrane GCs (GC-A–GC-G) have been discovered in various mammals, although it has been suggested that GC-D, localized to the olfactory epithelium of the rat, and GC-G, expressed in the intestine, lung, and skeletal muscle of the rat, are pseudogenes in the human (2). Ligands have been identified for three of the seven putative receptors: GC-A, atrial natriuretic peptide and brain natriuretic peptide; GC-B, C-type natriuretic peptide (CNP); and GC-C, heat-stable enterotoxins, guanylin, uroguanylin, and lymphoguanylin (1). The forms containing no apparent transmembrane segments, which exist as heterodimers, are associated with both the soluble and particulate fractions of cells. The major form appears to be an $\alpha 1\beta 1$ heterodimer, a receptor for nitric oxide (1).

Definition of the physiological roles of the various GCs has often relied on the use of genetic models or on the use of relatively specific inhibitors. Based on these studies, GC-A is known to regulate blood pressure, water, and electrolyte balance; to inhibit myocyte hypertrophy and fibrosis in the heart (3); and to regulate testosterone production (4). The normal function of GC-C remains unclear, although it is a signaling receptor for the heat-stable enterotoxins that cause an acute secretory diarrhea (3). GC-E and GC-F are localized to the photoreceptors, and mutations in GC-E cause impairments of vision in both mice and humans (3). Because GC-F is localized to the X chromosome, mutations in the gene may cause impairments of vision specifically in the male (3). GC-B is expressed in many different regions of the body, and the receptor has been strongly implicated as having a significant counterregulatory role to a variety of growth factors that promote cell proliferation, migration, and hypertrophy, in both cell culture and in a limited number of animal models. Mitogen-activated protein kinase cascades and Ca^{2+} signaling pathways appear as targets after GC-B activation (5, 6). Additionally, CNP/GC-B is known to induce differentiation of vascular smooth muscle cells, chondrocytes, and neuronal precursors (7–9). In general, however, the functions of GC-B have remained unclear, in part because specific inhibitors of the receptor-signaling pathway have not been available. Here, we disrupt the gene for this receptor and report phenotypes that suggest important functions for this receptor in skeletal growth and the maturation of female reproductive organs.

Methods

Generation of GC-B Null and GC-B Transgenic (TG) Mice. The murine GC-B gene (*Npr2*) was isolated from a 129S6/SvEvTac (129S6) mouse genomic library in a λFixII vector (Stratagene) (10). A targeting vector was constructed so that exons 3–7, which encode the C-terminal half of the extracellular ligand-binding domain and the transmembrane segment, were replaced by the neomycin resistance gene (*neo*). The vector was introduced into 129S6 strain-derived embryonic stem cells (SM-1) by electroporation at 230 V and 500 μF with a Gene Pulser (Bio-Rad). Seven clones were obtained after double selection with G418 (300 μg/ml) and 2′-fluoro-2′-deoxy-β-D-arabinofuranosyl-5-iodouracil (0.2 μM). One clone was determined to be appropriately targeted by Southern blot analysis with both 5′ and 3′ external probes (Fig. 7, which is published as supporting information on the PNAS web site). The clone was injected into blastocysts of C57BL/6 (B6) mice, which were then transferred to pseudopregnant females to generate chimeric males. Chimeric males with germline transmission of the knockout allele were bred to B6 females, and the line was maintained in a 129S6 × B6 hybrid genetic background.

TG mice with targeted expression of the GC-B2 isoform in growth-plate chondrocytes were generated. A 1.9-kb *Hin*dIII–*Eco*RI fragment of a β geo expression vector with promoter and enhancer regions of murine pro-α_1(II) collagen gene (*Col2a1*) (p3000i3020Col2a1-β geo; provided by B. de Crombrugghe, University of Texas M. D. Anderson Cancer Center, Houston) (11) was replaced with a 3.2-kb GC-B2 cDNA (10) to generate a TG construct. TG mice were generated in a B6 × SJL background as described in ref. 12.

Freely available online through the PNAS open access option.

Abbreviations: 129S6, 129S6/SvEvTac; B6, C57BL/6; cGKII, cGMP-dependent protein kinase II; CNP, C-type natriuretic peptide; GC, guanylyl cyclase; GH, growth hormone; IGF-I, insulin-like growth factor I; PCNA, proliferating cell nuclear antigen; TG, transgenic.

**To whom correspondence should be addressed at: Cecil H. and Ida Green Center for Reproductive Biology Sciences and Howard Hughes Medical Institute, University of Texas Southwestern Medical Center, 5323 Harry Hines Boulevard, Dallas, TX 75390-9051. E-mail: david.garbers@utsouthwestern.edu.

www.pnas.org/cgi/doi/10.1073/pnas.0407894101

Genotypes of mice were determined by Southern blot or PCR analyses by using genomic DNA isolated from tail tips. Animal care and all experiments were conducted as approved by the Institutional Animal Care and Use Committee of the University of Texas Southwestern Medical Center. The mice were kept on a 12-h light/dark cycle (light, 0600–1800 h) with free access to water and a standard mouse/rat chow diet, unless otherwise stated. Littermates were used as controls.

Primary Culture of Dermal Fibroblasts. Primary cultures of dermal fibroblasts were prepared from 8- to 12-wk-old mice as described in ref. 13. The cells were plated in DMEM (4.5 mg/ml glucose, Invitrogen) supplemented with 10% FBS, 500 units/ml penicillin, and 500 μg/ml streptomycin. The cells were passaged when they became 70–80% confluent and were used for experiments before the fifth passage.

RNA Isolation and Analysis. Total RNA was isolated from murine organs and primary fibroblast cultures with TRIzol reagent (Invitrogen), according to the supplier's instructions. Complementary DNA fragments of *Npr2* (exons 2–7), murine pro-α_1(X) collagen (*Col10a1*), murine Indian hedgehog (*Ihh*), and glyceraldehyde 3-phosphate dehydrogenase (*Gapdh*) were obtained by RT-PCR and subcloned into a pGEM-T Easy TA-cloning vector (Promega). Primers used for *Npr2*, *Col10a1*, and *Ihh* are listed in Table 1, which is published as supporting information on the PNAS web site. A mouse glyceraldehyde-3-phosphate dehydrogenase control amplimer set (Clontech) was used for *Gapdh*. Gene expression of *Npr2* or *Gapdh* was examined by Northern blot analysis with the cDNA fragments as probes.

RIA. cGMP levels were estimated by an RIA as described in ref. 14. Serum aldosterone and insulin-like growth factor I (IGF-I) concentrations were estimated by rat aldosterone and rat IGF-I RIA kits (Diagnostic Systems Laboratories, Webster, TX), respectively.

Skeletal and Histological Analyses. For skeletal analysis, mice were killed, skinned, eviscerated, and subjected to plain film radiography that was performed on a mammography unit in the Department of Radiology at the University of Texas Southwestern Medical Center.

For histological analysis, mice were perfused with 4% formaldehyde, freshly prepared from paraformaldehyde, in 0.1 M phosphate buffer (pH 7.4) under anesthesia, and tissues were then isolated and fixed by immersion in the same fixative for 24 h. Subsequent paraffin processing, embedding, and sectioning were performed by standard procedures described in refs. 15 and 16. Bone specimens were decalcified in 14% EDTA that was prepared in deoxypirocarbonate-treated water for 6 days before embedding in paraffin. Slices were made and stained with hematoxylin/eosin.

For immunohistochemical detection of proliferating cell nuclear antigen (PCNA), antigen retrieval was accomplished by boiling in citric acid; serial sections were then subjected to either anti-PCNA rabbit polyclonal antiserum (0.5 μg/ml) or normal rabbit serum with a VECTASTAIN ABC immunostaining kit (peroxidase, Vector Laboratories) and a DAB substrate (Vector Laboratories). The counterstaining was with Methyl Green (Vector Laboratories).

For radioisotopic *in situ* hybridization, ^{35}S-labeled sense and antisense probes were generated from the cDNA fragments by a Maxiscript kit (Ambion, Austin, TX). *In situ* hybridization was performed as described in ref. 17. Details are given in *Supporting Methods*, which is published as supporting information on the PNAS web site.

Review and photography of histologic sections were carried out on a Zeiss Axioplan 2i photomicroscope equipped with bright-field and incident angle dark-field illumination. Photomicrography was achieved by using this microscope and an Axiocam monochromatic charge-coupled device camera with a CRI RGB color filter (Zeiss). Images were captured by using OPENLAB 3.0.3 acquisition and analysis software and processed with PHOTOSHOP 5.5 (Adobe Systems, San Jose, CA).

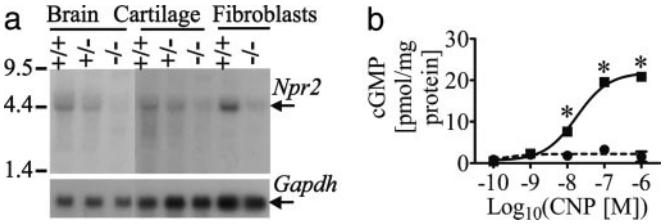

Fig. 1. No detectable GC-B mRNA expression or enzyme activity in mice with targeted disruption of the *Npr2* gene. (*a*) *Npr2* gene expression detected in the whole brain, growth-plate cartilage, and primary culture of dermal fibroblasts by Northern blot analysis (20 μg of total RNA per lane). *Gapdh* mRNA is shown in *Lower* as an internal control. (*b*) CNP-dependent increases of intracellular cGMP contents in dermal fibroblasts isolated from WT (■) and null (●) mice ($n = 3$). On the *x* axis, ''−10'' means vehicle-treated. *, $P < 0.001$ vs. null, by two-way ANOVA with Bonferroni's post hoc test.

Tibial Explant Culture. $Npr2^{+/+}$ and $Npr2^{-/-}$ neonates were killed under anesthesia at 1200 h. Tibiae were isolated and placed onto a 25-mm dish nitrocellulose filter (0.8-μm pore, Millipore) submerged in BGJb medium with Fitton–Jackson modification (Invitrogen) plus 0.1% BSA (Sigma), 100 units/ml penicillin, and 100 μg/ml streptomycin and then incubated at 37°C in a CO_2 incubator (5% CO_2) for 2–3 h. The medium was then changed to the medium with 1 μM CNP or the vehicle (0.5 mM sodium acetate); one tibia from each neonate was treated with CNP, and the other was treated with the vehicle. The tibiae were in culture for 6 days, and the medium was changed every other day. Photography was carried out by using an inverted microscope (SMZ1500, Nikon) equipped with a digital camera (DXM1200, Nikon), and measurements were performed with an image analysis system (ACT-1, Nikon).

Blood-Pressure Measurements. Blood pressure or pulse rate of mice was measured by a tail-cuff method with a blood-pressure monitor (Softron, Tokyo). Blood-pressure measurements and blood collection were accomplished in animals on normal-salt, high-salt, and low-salt diets (see *Supporting Methods*).

Statistics. All data are shown as mean ± SEM. Statistical analyses of data were performed with GRAPHPAD PRISM 3.00 for Windows (GraphPad, San Diego).

Results

Generation of GC-B Null Mice. We generated mice with a disrupted *Npr2* allele by gene-targeting (Fig. 7). *Npr2* mRNA levels in the brain or growth-plate cartilage were decreased by ≈50% in $Npr2^{+/-}$ mice relative to WT. In null animals, *Npr2* mRNA was not detected in the brain, growth-plate cartilage, or primary cultures of dermal fibroblasts (Fig. 1*a*). cGMP was not elevated by the addition of CNP to GC-B null fibroblasts (Fig. 1*b*). At 8 days of age, cGMP concentrations in the tail bone of $Npr2^{+/-}$ (15.3 ± 3.0 pmol/g of tissue, $n = 5$) and WT (14.0 ± 3.1, $n = 5$) mice were equivalent, but null mice contained significantly lower concentrations (3.8 ± 2.3, $n = 5$, $P < 0.05$ by ANOVA with Tukey's post hoc test). Given that CNP is expressed in the growth-plate cartilage, the cGMP levels do not reflect basal GC-B activity without CNP binding but an activity augmented by CNP binding. Analysis of 31 intercrosses between heterozygous 129S6 × B6 hybrids yielded the following genotype ratios: (*i*) at

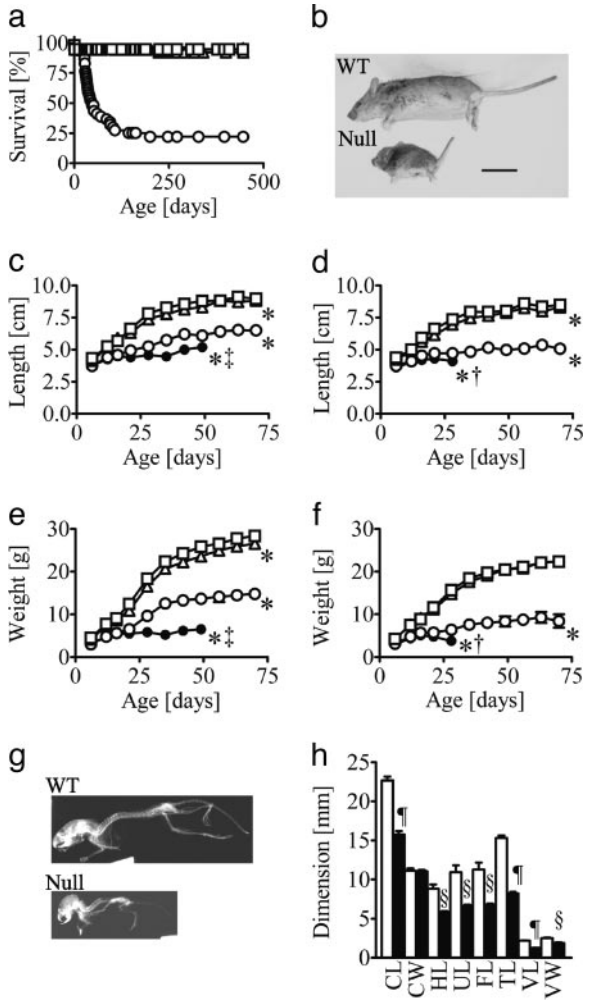

Fig. 2. Dwarfism and early mortality of GC-B-null mice. (*a*) The longevity of $Npr2^{-/-}$ mice (○, $n = 48$) is shorter than that of $Npr2^{+/+}$ (□, $n = 56$) or $Npr2^{+/-}$ (△, $n = 107$) mice ($P < 0.0001$, by the Kaplan–Meier method). (*b*) Gross appearance of 90-day-old WT and null females. (Scale bar, 2.5 cm.) (*c*) Male growth curves in nasoanal length: $Npr2^{+/+}$, □, $n = 9$; $Npr2^{+/-}$, △, $n = 10$; $Npr2^{-/-}$ surviving beyond 100 days (group A), ○, $n = 7$; $Npr2^{-/-}$ dying before 100 days (group B), ●, $n = 8$. *, $P < 0.0001$ vs. $Npr2^{+/+}$; †, $P < 0.05$; ‡, $P < 0.01$ vs. $Npr2^{-/-}$ (group A), by two-way ANOVA. (*d*) Female growth curves in nasoanal length: $Npr2^{+/+}$, □, $n = 11$; $Npr2^{+/-}$, △, $n = 9$; $Npr2^{-/-}$ (group A), ○, $n = 5$; $Npr2^{-/-}$ (group B), ●, $n = 7$. (*e* and *f*) Growth curves of males (*e*) and females (*f*) in body weight. (*g* and *h*) Plain x-ray analysis of 30-day-old WT and GC-B-null mice. Shown are photos of representative cases (*g*) and bone dimensions of $Npr2^{+/+}$ (open bars) and $Npr2^{-/-}$ (filled bars) mice (*h*) ($n = 3$). CL, nasooccipital length of the skull; CW, interparietal width of the skull; HL, humeral length; UL, ulnar length; FL, femoral length; TL, tibial length; VL, vertebral length; VW, vertebral width. The data of VL and VW are means of the first through fifth lumbar vertebrae. §, $P < 0.05$; ¶, $P < 0.01$ vs. $Npr2^{+/+}$, by Student's *t* test.

birth ($n = 255$): $Npr2^{+/+}$, 1.0; $Npr2^{+/-}$, 1.6; and $Npr2^{-/-}$, 0.7; and (*ii*) at weaning ($n = 242$): $Npr2^{+/+}$, 1.0; $Npr2^{+/-}$, 1.7; and $Npr2^{-/-}$, 0.7. These values are not significantly different from Mendelian expectations (χ^2 test). In the hybrid background (Fig. 2*a*), >90% of null mice survived until weaning, but 75% died before 100 days of age. The median survival time was 47 days (Kaplan–Meier method). Longevity of $Npr2^{-/-}$ mice surviving beyond 100 days, however, was not different from that of WT and $Npr2^{+/-}$ mice.

$Npr2^{-/-}$ animals showed self-clasping and priapism, suggesting neuronal disorders. Self-clasping is a movement disorder first described in distonic mice (dystonia musculorum) with axonal degeneration (18) in which a mouse flexes one or both hind limbs to the trunk when lifted by the tail. Normal mice extend both hind limbs. Priapism is forced penile erection and is commonly observed in patients with a spinal injury (19). Despite these phenotypes, no histological abnormalities were seen in the brain or spinal cord of $Npr2^{-/-}$ mice.

Female $Npr2^{-/-}$ mice were sterile (described later). One male mouse that survived beyond 100 days was fertile. The male did not suffer from priapism until it had successfully mated with female mice (described later).

Dwarfism in GC-B Null Mice. Null mice could be distinguished from $Npr2^{+/+}$ or $Npr2^{+/-}$ mice several days after birth by their smaller body size. Dwarfism became more prominent as null mice grew older (Fig. 2 *b–f*); they retained a significantly shorter naso-anal length and smaller body weight than WT mice from day 6 through day 70. Null mice that survived beyond 100 days (group A) were 60–70% in nasoanal length and ≈50% in body weight relative to WT mice (Fig. 2 *c–f*). After weaning, GC-B null mice that died before 100 days (group B) ceased to grow, and body weight began to decrease, whereas group A null mice continued to grow (Fig. 2 *c–f*). $Npr2^{+/-}$ males were significantly smaller in both nasoanal length and body weight than WT males, although the difference was small (Fig. 2 *c* and *e*). Nasoanal length of $Npr2^{+/-}$ females was significantly smaller than that of WT females, but there were no significant differences in the body weights of $Npr2^{+/+}$ and $Npr2^{+/-}$ females (Fig. 2 *d* and *f*). Analysis of skeletons by plain x-ray films showed that longitudinal growth of long bones in limbs or vertebrae and skull-base growth in nasooccipital dimension were impaired; lateral growth of the calvarium was not altered (Fig. 2 *g* and *h*). Elongation of lower or upper incisors was seen frequently in $Npr2^{-/-}$ mice of group B (Fig. 2*g*) but not in group A. Discrepancy in growth between the calvarium and skull base appeared to result in misalignment between the upper and lower incisors, leading to their elongation. Cutting of the incisors and providing powdered diet was required eventually.

We investigated the histology of tibiae from 8-day-old pups to define the basis of the dwarf phenotype. The growth-plate cartilage consists of four distinct layers: periarticular, columnar proliferating, prehypertrophic, and hypertrophic chondrocyte (20) (Fig. 3*a*). The columnar proliferating, prehypertrophic, and hypertrophic chondrocyte layers were thinner in null mice than in WT mice (Fig. 3*a*). To determine whether proliferation of chondrocytes was impaired, we examined the expression of PCNA in the tibial growth plate by immunohistochemistry. PCNA-positive chondrocytes were detected in the periarticular through prehypertrophic chondrocyte layers in tibial growth plates of all genotypes, and the intensity of the signal was similar (Fig. 3*b*). However, terminally differentiated hypertrophic chondrocytes, identified by failure to express PCNA, were almost completely absent in null animals (Fig. 3*b*). We then investigated the expression of the *Npr2*, *Col10a1*, and *Ihh* genes in the tibial growth plate by *in situ* hybridization. Pro-α_1(X) collagen is an important cartilage matrix protein and a molecular marker for hypertrophic chondrocytes. The *Ihh* gene is expressed in prehypertrophic chondrocytes that have committed terminal differentiation into hypertrophic chondrocytes (21). *Npr2* gene expression was evident in the columnar proliferating and prehypertrophic chondrocyte layers in WT tibia but not in null tibia (Fig. 3*c*). *Col10a1* gene expression was evident in the prehypertrophic and hypertrophic chondrocyte layers of both WT and null tibiae, but the *Col10a1*-positive layer was considerably thinner in null tibia (Fig. 3*c*). *Ihh* gene expression was seen only in the prehypertrophic chondrocyte layer of both WT and null tibiae. The intensity of the signal was similar in WT and null animals, but the *Ihh*-positive layer was thinner in null animals

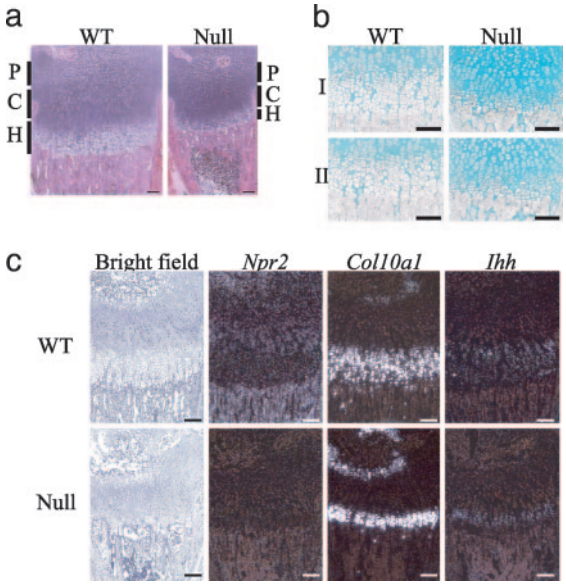

Fig. 3. Growth-plate histology of 8-day-old WT and GC-B-null mice. (*a*) Hematoxylin/eosin staining of proximal growth-plate sections of tibiae. Periarticular (P), columnar proliferating (C), and prehypertrophic and hypertrophic (H) chondrocyte layers are indicated. (*b*) Immunohistochemical detection of PCNA in the tibial growth plate. I, with anti-PCNA rabbit serum; II, with nonimmune rabbit serum. (*c*) Detection of *Npr2*, *Col10a1*, and *Ihh* gene expression by *in situ* hybridization. (Scale bars, 0.1 mm.)

(Fig. 3*c*). It has been reported that CNP stimulates the secretion of growth hormone (GH) from rat pituitary gland-derived GH3 cells (22). We have detected high expression of *Npr2* mRNA in the murine pituitary gland (10). Defects of GH/GH receptor signaling are major causes of dwarfism in humans and mice. At 70–120 days of age, serum IGF-I levels, an excellent indicator of GH secretion (23), were lower in $Npr2^{-/-}$ mice than in $Npr2^{+/+}$ or $Npr2^{+/-}$ mice. [Females: $Npr2^{+/+}$, 407 ± 46 ng/ml; $Npr2^{+/-}$, 471 ± 22; $Npr2^{-/-}$, 213 ± 66 ($P < 0.05$ vs. $Npr2^{+/+}$, $P < 0.05$ vs. $Npr2^{+/-}$, by ANOVA with Tukey's post hoc test, $n = 4$). Males: $Npr2^{+/+}$, 388 ± 42; $Npr2^{+/-}$, 358 ± 54; $Npr2^{-/-}$, 275 ± 31, (no significant differences, $n = 5$).

To confirm that impaired skeletal growth is not a secondary effect to GH secretion or other peripheral hormone alterations, we studied tibial explants in culture. The length of cartilaginous primordia was not different as a function of genotype at the beginning of the culture (Fig. 4*b*). After 6 days in culture, increases in length of cartilaginous primordia were evident in all genotypes, but lengths in WT increased faster (Fig. 4). The addition of 1 μM CNP significantly enhanced the increase in WT, but not in null tibiae (Fig. 4*b*). The calcified ossification center was significantly shorter in null tibiae compared with WT tibia (Fig. 4). Increases in the length of the ossification centers were not significant during the culture with or without 1 μM CNP (Fig. 4*b*).

GC-B2 Overexpression in Growth-Plate Chondrocytes. GC-B2 retains CNP binding and basal GC activity but fails to respond to CNP and thus serves as a dominant negative isoform with respect to CNP-dependent increases of cGMP (10). Overexpression of GC-B2 may increase a basal GC-B activity without CNP binding, but it inhibits activation of GC-B by CNP binding (10). To see whether the activation of GC-B by CNP binding is important for progression of the endochondral ossification, we generated TG mice that overexpress GC-B2 in growth-plate chondrocytes (lines 25-4, 26-2, and 29-7). At 10 days of age, GC-B2 mRNA expression was barely detected in the WT growth plate but was equivalent to GC-B1 mRNA expression in the growth plate of a GC-B2 TG mouse of line 29-7 (Fig. 5*a*); GC-B2 mRNA levels were highest in line 29-7 of three lines. At 10 days of age, cGMP levels of tail bones were decreased by 25% in TG mice (line 29-7, 14.2 ± 0.6 pmol/g of tissue, $n = 6$, $P < 0.05$ by Student's t test) relative to WT mice (19.4 ± 2.0, $n = 5$). This observation is consistent with the fact that intracellular cGMP levels were lower in COS-7 cells expressing GC-B1 and GC-B2 at a 1:1 ratio than in the cells expressing only GC-B1, where CNP was 10 nM through 1 μM (10). TG mice (line 29-7) were significantly shorter in nasoanal length than WT mice of both sexes (Fig. 5*b*). In the other two lines, nasoanal length also was reduced but by a lesser magnitude.

Blood-Pressure Regulation. Mice placed on normal-salt (0.7% NaCl), high-salt (8% NaCl), or low-salt (0.008% NaCl) diets did not show significant differences in blood pressure as a function of genotype (Table 2, which is published as supporting information on the PNAS web site), other than systolic blood pressure being lower in the heterozygous animals [95 ± 1 mmHg (1 mmHg = 133 Pa), $n = 5$] relative to the WT mice (106 ± 2, $n = 5$) on the normal-salt diet. Serum aldosterone concentrations decreased on the high-salt diet and increased on the low-salt diet, but all such changes occurred independent of genotype, other

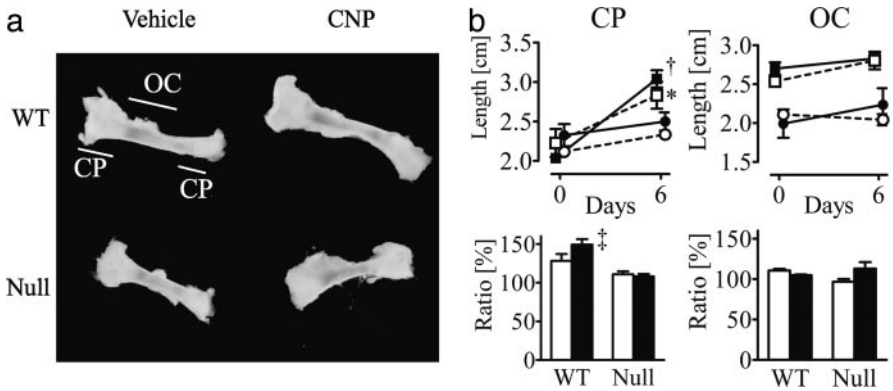

Fig. 4. Tibial explant culture from neonates. (*a*) Tibial explants after 6-day culture with vehicle or 1 μM CNP. CP, cartilaginous primordium; OC, calcified ossification center. (*b*) Longitudinal growth of CPs (sum of CPs on both ends) and OC of tibial explants during the culture. The length of vehicle-treated WT (□) and null (○) explants and CNP-treated WT (■) and null (●) explants are shown in *Upper*. Ratios of final to initial length in vehicle- and CNP-treated groups are shown by open and filled bars, respectively, in *Lower*. *, $P < 0.05$; †, $P < 0.01$ vs. day 0 in each group, by two-way ANOVA with Bonferroni's post hoc test ($n = 5$); ‡, $P < 0.05$ vs. vehicle-treated in each genotype, by ANOVA with Tukey's post hoc test ($n = 5$).

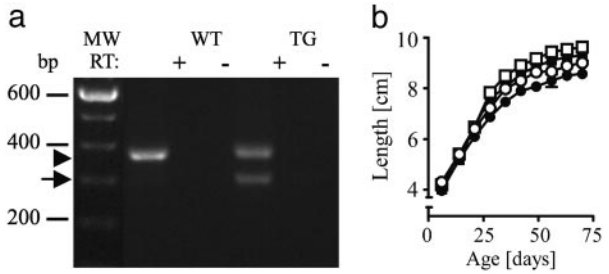

Fig. 5. Transgene expression and phenotype of GC-B2 TG mice. (*a*) GC-B1 and GC-B2 mRNA expression in the growth-plate cartilage detected by RT-PCR. Selected molecular weight (MW) markers are shown on the left in bp; bands of GC-B1 and GC-B2 are indicated by an arrowhead and an arrow, respectively. Reactions with (+) or without (−) a reverse transcriptase of RNA isolated from the growth-plate cartilage of WT and GC-B2 TG mice are used for PCR as templates. (*b*) Growth of GC-B2 TG mice in nasoanal length. Data of WT females (○), TG females (●), WT males (□), and TG males (■) are shown ($n = 5$). TG mice are significantly ($P < 0.0001$, by two-way ANOVA) shorter than WT mice in each sex.

than a blunting in serum aldosterone levels in response to the low-salt diet in heterozygotes (2,388 ± 651 pg/ml vs. 4,741 ± 265 in WT, $n = 4$).

Reproductive Organs. Because all females were sterile, we determined the nature of the defect. At 100 days of age, the uterus failed to show normal development in null mice (group A; Fig. 6 *a* and *b*). The uterine horn was string-like, with a very thin endometrium and myometrium relative to WT animals; the null uterus also lacked the secondary glandular structures of the WT uterus (Fig. 6 *c* and *d*). In addition, ovarian size was smaller in

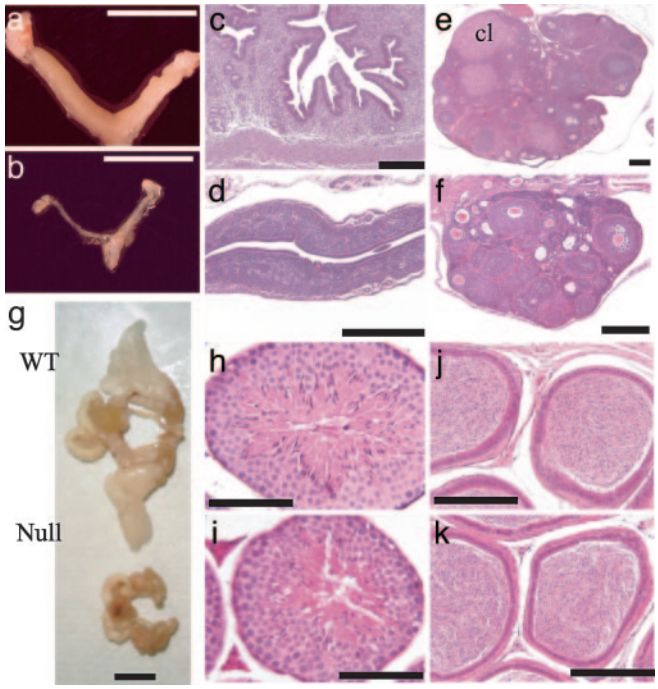

Fig. 6. Phenotypes of reproductive organs. (*a–f*) Gross appearance of female reproductive organs (*a* and *b*) and histology of uteri (*c* and *d*) and ovaries (*e* and *f*) from WT (*a*, *c*, and *e*) and null (*b*, *d*, and *f*) mice with hematoxylin/eosin staining. A corpora luteum (cl) is indicated in e. (*g–k*) Gross appearance of male reproductive organs (*g*) and histology of testes (*h* and *i*) and epididymi (*j* and *k*) from WT (*h* and *j*) and null (*i* and *k*) mice. (Scale bars: *a*, *b*, and *g*, 1 cm; *c–f* and *h–k*, 0.2 mm.)

$Npr2^{-/-}$ females (Fig. 6 *a*, *b*, *e*, and *f*). Well developed corpora lutea were present in WT mice, whereas only primordial through secondary antral follicles existed in $Npr2^{-/-}$ ovaries (Fig. 6 *e* and *f*). No estrus cycles were apparent, based on the cytology of vaginal smears. In contrast, male reproductive organs, including testes, epididymi, and seminal vesicles, were similar in size in null and WT animals (Fig. 6*g*). Histological analysis of testes and epididymi showed no structural abnormalities in $Npr2^{-/-}$ males. Terminally developed spermatids were present in tubules of testes and epididymi (Fig. 6 *h–k*).

Discussion

Endochondral ossification is responsible for the longitudinal growth of long bones in limbs and vertebrae and takes place at the growth-plate cartilage located at both ends of the bones (20). Chondrocytes begin to proliferate in the periarticular chondrocyte layer and multiply by forming columns in the columnar proliferating chondrocyte layer. They shift to differentiation at the prehypertrophic chondrocyte layer and become hypertrophic chondrocytes that synthesize cartilage matrix in the hypertrophic chondrocyte layer. The cartilage tissue is then transformed into bone tissue by chondroclasts/osteoclasts and by osteoblasts recruited during blood-vessel invasion. Histological analysis of tibiae from 8-day-old $Npr2^{-/-}$ pups suggests that differentiation is the prominently impaired step of endochondral ossification. Mice lacking CNP ($Nppc^{-/-}$ mice) that exhibit a skeletal dwarfism have the same growth-plate histology as $Npr2^{-/-}$ mice; the periarticular, columnar proliferating, and hypertrophic chondrocyte layers are reduced in thickness (24). Expression of the *Nppc* gene is detected in the columnar proliferating and prehypertrophic chondrocyte layers in murine tibia (24), the same regions of *Npr2* expression. Disruption of the gene for cGMP-dependent protein kinase II (cGKII) (*Prkg2*), an effecter molecule downstream of GC-B/cGMP signaling, predominantly detected in the columnar proliferating and prehypertrophic chondrocyte layers of the murine growth plate, also results in dwarfism because of impaired endochondral ossification (25). During the course of this study, mutations in the human *NPR2* gene were reported to cause acromesomelic dysplasia, type Maroteaux, a type of skeletal dysplasia (26). Therefore, the CNP/GC-B/cGKII cascade appears critical for the proper progression of endochondral ossification through control of chondrocyte differentiation. Reduction of naso-anal length of GC-B2 TG mice suggests that a CNP-dependent increase of GC-B/cGKII signaling is important for the progression of endochondral ossification. The growth of the calvarium, which depends on membranous ossification, was not altered in $Npr2^{-/-}$, $Nppc^{-/-}$, or $Prkg2^{-/-}$ mice, suggesting that the CNP/GC-B/cGKII pathway selectively regulates endochondral ossification. A thick layer of a mixture of proliferating and hypertrophic chondrocytes was observed in $Prkg2^{-/-}$ mice (25), instead of the discrete, thin hypertrophic chondrocyte layer seen in $Nppc^{-/-}$ or $Npr2^{-/-}$ mice. The difference in growth-plate histology raises the possibility that there are signaling pathways converging on cGKII other than the CNP/GC-B/cGMP pathway. Impaired growth of $Npr2^{-/-}$ tibial explants indicates that the lack of GC-B in the growth plate is a primary cause of the impaired skeletal growth of $Npr2^{-/-}$ mice. That serum IGF-I levels were relatively lower in null mice than in WT mice reserves a possible involvement of pituitary GC-B signaling in the skeletal growth.

It has been reported that a reduction in size or ventral shift of the foramen magnum of the skull causes compression of the medulla oblongata and ultimately leads to death by respiratory arrest in some achondroplasia patients (27). In $Npr2^{-/-}$ mice, impaired growth of the skull base may cause compression of the medulla oblongata and early death. At 21 days of age, group B $Npr2^{-/-}$ mice were already significantly smaller than group A null mice (Fig. 2 *c* and *d*), suggesting that a smaller skull base is

related to the early mortality in group B *Npr2*$^{-/-}$ mice. Some *Npr2*$^{-/-}$ mice, however, died with tonic-clonic seizure attacks. This observation may suggest that GC-B signaling controls neuronal activities in combination with the self-clasping and priapism observed in *Npr2*$^{-/-}$ mice.

In the human *NPR2* gene, a GT microsatellite repeat polymorphism exists within the second intron, and the $(GT)_{11}$ allele significantly associates with essential hypertension (28). We did not see significant differences in blood pressure or pulse rate in *Npr2*$^{+/+}$ and *Npr2*$^{-/-}$ mice after a number of salt regimens (Table 2). The regulation of aldosterone secretion by salt intake appears maintained in *Npr2*$^{-/-}$ mice.

Apparent normal spermatogenesis and accessory organ structure in the male suggest that the major cause of male sterility is not associated with the reproductive organs but that abnormalities in the neuronal control of penile erection could be a cause. GC-B expression is detected in the rabbit corpus cavernosum, and CNP-dependent increases of cGMP result in relaxation of the corpus cavernosum smooth muscle, which then leads to penile erection (29). Thus, the priapism seen in the absence of GC-B appears to support the above report. In the female, sterility is caused by failure to properly develop functional ovaries or uteri. We have shown that the *Npr2* expression level is quite high in murine ovaries (10), and *Nppc* mRNA expression and CNP are detected in murine ovaries (30, 31). *Nppc* and *Npr2* genes are expressed in granulosa cells of follicles and thecal-interstitial cells of rat ovaries (30, 32). It has been reported that 8-bromo-cGMP can protect ovarian follicles from atresia and promote growth (33). In combination with observations that no corpora lutea and no estrus cycling were seen in null mice, the CNP/GC-B/cGMP system appears essential for the growth and maturation of ovarian follicles. It has been shown that not locally produced but circulating IGF-I is essential for the growth and development of the uterus (34); low serum IGF-I levels in female *Npr2*$^{-/-}$ mice might be another cause of the immature uterus. We detected *Npr2* gene expression in the murine uterus, and the expression level was higher than in ovaries (10), suggesting direct effects of signaling through GC-B on uterine development.

In conclusion, our investigation suggests that CNP-dependent augmentation of GC-B signaling is critical for normal endochondral ossification. Signaling through this receptor may also be important for the maturation of female reproductive organs.

We thank Ms. Elizabeth Lummus and Ms. Rebecca J. Varley for technical assistance; Dr. Orhan K. Oz and Mr. Curtis Chaney (Department of Radiology, University of Texas Southwestern Medical Center) for help with the plain x-ray analysis; the University of Texas Southwestern Medical Center Molecular Pathology Core staff for histological expertise; Dr. Patricia A. Preisig (Department of Internal Medicine, University of Texas Southwestern Medical Center) for the measurement of electrolyte concentrations; and Dr. Ted D. Chrisman for valuable discussions. This work was supported in part by an award from the Sandler Program for Asthma Research (to D.L.G.), the Howard Hughes Medical Institute, and the Cecil H. and Ida Green Center for Reproductive Biology Sciences.

1. Garbers, D. L. & Lowe, D. G. (1994) *J. Biol. Chem.* **269,** 30741–30744.
2. Manning, G., Whyte, D. B., Martinez, R., Hunter, T. & Sudarsanam, S. (2002) *Science* **298,** 1912–1934.
3. Wedel, B. & Garbers, D. L. (2001) *Annu. Rev. Physiol.* **63,** 215–233.
4. Pandey, K. N., Oliver, P. M., Maeda, N. & Smithies, O. (1999) *Endocrinology* **140,** 5112–5119.
5. Chrisman, T. D. & Garbers, D. L. (1999) *J. Biol. Chem.* **274,** 4293–4299.
6. Abbey, S. E. & Potter, L. R. (2002) *J. Biol. Chem.* **277,** 42423–42430.
7. Doi, K., Ikeda, T., Itoh, H., Ueyama, K., Hosoda, K., Ogawa, Y., Yamashita, J., Chun, T. H., Inoue, M., Masatsugu, K., *et al.* (2001) *Arterioscler. Thromb. Vasc. Biol.* **21,** 930–936.
8. Suda, M., Tanaka, K., Yasoda, A., Komatsu, Y., Chusho, H., Miura, M., Tamura, N., Ogawa, Y. & Nakao, K. (2002) *J. Bone Miner. Metab.* **20,** 136–141.
9. Simpson, P. J., Miller, I., Moon, C., Hanlon, A. L., Liebl, D. J. & Ronnett, G. V. (2002) *J. Neurosci.* **22,** 5536–5551.
10. Tamura, N. & Garbers, D. L. (2003) *J. Biol. Chem.* **278,** 48880–48889.
11. Zhou, G., Garofalo, S., Mukhopadhyay, K., Lefebvre, V., Smith, C. N., Eberspaecher, H. & de Crombrugghe, B. (1995) *J. Cell Sci.* **108,** 3677–3684.
12. Kishimoto, I., Rossi, K. & Garbers, D. L. (2001) *Proc. Natl. Acad. Sci. USA* **98,** 2703–2706.
13. Bradshaw, A. D., Francki, A., Motamed, K., Howe, C. & Sage, E. H. (1999) *Mol. Biol. Cell* **10,** 1569–1579.
14. Domino, S. E., Tubb, D. J. & Garbers, D. L. (1991) *Methods Enzymol.* **195,** 345–355.
15. Woods, A. E. & Ellis, R. C. (1996) *Laboratory Histopathology: A Complete Reference* (Churchill Livingstone, New York).
16. Shehan, D. C. & Hrapchak, B. B. (1980) *Theory and Practice of Histotechnology* (Battelle, Columbus, OH).
17. Shelton, J. M., Lee, M. H., Richardson, J. A. & Patel, S. B. (2000) *J. Lipid Res.* **41,** 532–537.
18. Duchem, L. W. & Strich, S. J. (1964) *Brain* **87,** 367–378.
19. Marson, L. & McKenna, K. E. (1990) *Brain Res.* **515,** 303–308.
20. Howell, D. S. & Dean, D. D. (1992) *Disorders of Bone and Mineral Metabolism* (Raven, New York).
21. Vortkamp, A., Lee, K., Lanske, B., Segre, G. V., Kronenberg, H. M. & Tabin, C. J. (1996) *Science* **273,** 613–622.
22. Shimekake, Y., Ohta, S. & Nagata, K. (1994) *Eur. J. Biochem.* **222,** 645–650.
23. Baker, J., Liu, J. P., Robertson, E. J. & Efstratiadis, A. (1993) *Cell* **75,** 73–82.
24. Chusho, H., Tamura, N., Ogawa, Y., Yasoda, A., Suda, M., Miyazawa, T., Nakamura, K., Nakao, K., Kurihara, T., Komatsu, Y., *et al.* (2001) *Proc. Natl. Acad. Sci. USA* **98,** 4016–4021.
25. Pfeifer, A., Aszodi, A., Seidler, U., Ruth, P., Hofmann, F. & Fassler, R. (1996) *Science* **274,** 2082–2086.
26. Bartels, C. F., Bukulmez, H., Padayatti, P., Rhee, D. K., van Ravenswaaij-Arts, C., Pauli, R. M., Mundlos, S., Chitayat, D., Shih, L. Y., Al-Gazali, L. I., *et al.* (2004) *Am. J. Hum. Genet.* **75,** 27–34.
27. Gordon, N. (2000) *Brain Dev.* **22,** 3–7.
28. Rehemudula, D., Nakayama, T., Soma, M., Takahashi, Y., Uwabo, J., Sato, M., Izumi, Y., Kanmatsuse, K. & Ozawa, Y. (1999) *Circ. Res.* **84,** 605–610.
29. Kim, S. Z., Kim, S. H., Park, J. K., Koh, G. Y. & Cho, K. W. (1998) *J. Urol.* **159,** 1741–1746.
30. Jankowski, M., Reis, A. M., Mukaddam-Daher, S., Dam, T. V., Farookhi, R. & Gutkowska, J. (1997) *Biol. Reprod.* **56,** 59–66.
31. Huang, H., Acuff, C. G. & Steinhelper, M. E. (1996) *Am. J. Physiol.* **271,** H1565–H1575.
32. Noubani, A., Farookhi, R. & Gutkowska, J. (2000) *Endocrinology* **141,** 551–559.
33. McGee, E., Spears, N., Minami, S., Hsu, S. Y., Chun, S. Y., Billig, H. & Hsueh, A. J. (1997) *Endocrinology* **138,** 2417–2424.
34. Sato, T., Wang, G., Hardy, M. P., Kurita, T., Cunha, G. R. & Cooke, P. S. (2002) *Endocrinology* **143,** 2673–2679.